

# Nanoscale Simulation of the Thylakoid Membrane Response to Extreme Temperatures

Josh Vermaas V<sup>1</sup>, Martin Kulke<sup>1</sup>, Sarathi Weraduwege M<sup>2</sup>, and Thomas Sharkey<sup>1</sup>

<sup>1</sup>Michigan State University Department of Biochemistry and Molecular Biology

<sup>2</sup>MSU-DOE Plant Research Laboratory

February 7, 2023

## Abstract

The thylakoid membrane is in a temperature-sensitive equilibrium that shifts repeatedly during the life cycle in response to ambient temperature or solar irradiance. Plants respond to seasonal temperature by changing their thylakoid lipid composition, while a more rapid mechanism for short-term heat exposure is required. The emission of the small organic molecule isoprene has been postulated as one such possible rapid mechanism. The protective mechanism of isoprene is not known, but some plants emit isoprene during periods of high-temperature stress. In this work, we investigate the dynamics and structure for lipids within a thylakoid membrane at different temperatures and varied isoprene content using classical molecular dynamics simulations. The results are compared with experimental findings from across the literature for temperature-dependent changes in the lipid composition and shape of thylakoids. We find that the surface area, volume, and flexibility of the membrane, as well as the lipid diffusion, increase with temperature, while the membrane thickness decreases. Saturated thylakoid 34:3 glycolipids derived from eukaryotic synthesis pathways exhibit significantly different dynamics than lipids from prokaryotic synthesis paths, which could explain the upregulation of specific lipid synthesis pathways at different temperatures. Increasing isoprene concentration was not observed to have a significant thermoprotective effect on the thylakoid membranes, and that isoprene readily permeated the membrane models tested here.

# Nanoscale Simulation of the Thylakoid Membrane Response to Extreme Temperatures

Martin Kulke,<sup>†</sup> Sarathi M Weraduwege,<sup>‡,¶</sup> Thomas D Sharkey,<sup>‡</sup> and Josh  
V Vermaas<sup>\*,†</sup>

<sup>†</sup>*MSU-DOE Plant Research Laboratory and Department of Biochemistry and Molecular  
Biology, Michigan State University, 612 Wilson Rd, East Lansing, MI 48824, United States  
of America.*

<sup>‡</sup>*MSU-DOE Plant Research Laboratory, Michigan State University, 612 Wilson Rd, East  
Lansing, MI 48824, United States of America.*

<sup>¶</sup>*Current address: Bishop's University, 2600 Rue College, Sherbrooke, QC J1M 1Z7,  
Canada.*

E-mail: [vermaasj@msu.edu](mailto:vermaasj@msu.edu)

## Abstract

The thylakoid membrane is in a temperature-sensitive equilibrium that shifts repeatedly during the life cycle in response to ambient temperature or solar irradiance. Plants respond to seasonal temperature by changing their thylakoid lipid composition, while a more rapid mechanism for short-term heat exposure is required. The emission of the small organic molecule isoprene has been postulated as one such possible rapid mechanism. The protective mechanism of isoprene is not known, but some plants emit isoprene during periods of high-temperature stress. In this work, we investigate the dynamics and structure for lipids within a thylakoid membrane at different temperatures and varied isoprene content using classical molecular dynamics simulations. The results are compared with experimental findings from across the literature for temperature-dependent changes in the lipid composition and shape of thylakoids. We find that the surface area, volume, and flexibility of the membrane, as well as the lipid diffusion, increase with temperature, while the membrane thickness decreases. Saturated thylakoid 34:3 glycolipids derived from eukaryotic synthesis pathways exhibit significantly different dynamics than lipids from prokaryotic synthesis paths, which could explain the upregulation of specific lipid synthesis pathways at different temperatures. Increasing isoprene concentration was not observed to have a significant thermoprotective effect on the thylakoid membranes, and that isoprene readily permeated the membrane models tested here.

## Introduction

Plants must constantly adjust to changes in environmental temperature caused by seasons, sun intensity, and day/night cycles. Maintaining the efficiency of the photosynthetic reaction center inside the chloroplast during temperature fluctuations is critical for survival.<sup>1</sup> The photosynthetic machinery of plants is composed of membrane embedded complexes. Within the chloroplast, the photosynthetic reaction center and its antenna complexes are embedded in the grana formed by stacked thylakoid membranes,<sup>2,3</sup> consisting of glycolipids, phospholipids, isoprenoids and proteins.<sup>4</sup> The granas are connected in the chloroplast stroma through unstacked thylakoid membranes. The main lipids in these thylakoids are the glycolipids MGDG (monogalactosyldiacylglycerol) and DGDG (digalactosyldiacylglycerol) that account for ~57% and ~27% of the total lipid content, respectively.<sup>5</sup> The ratio between MGDG and the other lipids determines the thylakoid ultrastructure and is strictly regulated.<sup>6,7</sup> While MGDG does prefer a hexagonal-II phase, the other lipids DGDG, SQDG (Sulfoquinovosyl diacylglycerols) and PG (phosphatidylglycerol) form lamellar bilayer phases.<sup>8,9</sup> The anionic phospholipid PG is essential for the function of photosystem (PS) II.<sup>10</sup> SQDG can partially replace for PG's photosynthetic role, and plant regulatory mechanisms keep the total amount of PG and SQDG constant.<sup>11,12</sup> Thylakoids also contain traces of PI (Phosphatidylinositol), an important signaling lipid, which communicates different stresses by phosphorylating various positions on the inositol ring.<sup>13</sup>

Not all lipids contained in the thylakoids are synthesized entirely via the prokaryotic pathway maintained within the chloroplast. Specifically, lipids with 18 carbon fatty acid chains at the sn-2 position are synthesized via the eukaryotic pathway in the endoplasmic reticulum (ER).<sup>14</sup> The chloroplast genome synthesizes lipids whose fatty acids have 16 carbon chains in the sn-2 position, distinguishing them from the eukaryotic pathway. The transport mechanism between ER and chloroplast is not fully understood, but presumably diacylglycerol, PC or PA is transported to the chloroplast and further synthesized into PG and PI glycolipids.<sup>15</sup>

The lipid dynamics and structure for thylakoid membranes respond to changing environmental temperatures. The nanoscale response to temperature change thylakoid structure and dynamics overall, which consequently affects photosynthesis.<sup>16,17</sup> At higher temperatures the grana is reorganized with thylakoid membranes destacking<sup>18</sup> resulting in a dissociation of the light harvesting units from PS II.<sup>19</sup> This also potentially alters the reaction center of PS II,<sup>20</sup> inhibiting electron transfer between  $Q_A$  and  $Q_B$ <sup>21</sup> and resulting in an energy imbalance.<sup>22</sup> At higher temperature, the fluidity of the thylakoid membrane increases, leading to an increase in membrane permeability<sup>23</sup> that allows protons to leak through, lowering the potential proton motive force built up by photosynthetic action. Conversely, at temperatures below 13°C, the volume occupied by thylakoids decreases,<sup>24,25</sup> the total number of granas reduces,<sup>26-28</sup> and the granas may also unstack,<sup>29</sup> leading to the degradation of thylakoid membranes at longer incubation times.<sup>30</sup> Below the freezing point, thylakoids can phase-transfer to the gel phase, drastically reducing the flexibility and fluidity. Although the phase transition point for the thylakoid is much lower than for other membrane types,<sup>31</sup> ice crystal formation disrupts the membrane structure and leads to wavelike deformations.<sup>32</sup>

Thus, temperature variation requires a response from the plant to protect the photosynthetic reaction center. Across seasonal variation and diurnal temperature swings, the plant has hours to adjust the lipid composition in the thylakoid membranes. The fluidity of the membrane at higher temperatures is decreased by saturating the lipid acyl chains and increasing the isoprenoid content.<sup>33-35</sup> Conversely, lipid acyl chains are desaturated at low temperature.<sup>36,37</sup> Furthermore, the MGDG/DGDG ratio and the PG content generally decrease at low temperatures, varying depending on plant species.<sup>36-38</sup> Higher glycosylated lipids tri- and tetragalactosyldiacylglycerol (TGDG, TeDG) accumulate during freezing conditions.<sup>6</sup>

In the short term, plants have to endure localized high temperatures from intense sunlight. In this case, changing the membrane composition may not be metabolically fast enough or energetically not advantageous. Plants respond with heat shock proteins (HSP) that act as

chaperons to quality control protein folds.<sup>22</sup> Another mechanism discussed in the literature is the expression of isoprene.<sup>39,40</sup> While the function of isoprene within plant tissues remains unresolved, current hypotheses include preventing oxidative stress or protecting the photosynthetic reaction center from thermal damage.<sup>41–43</sup> Experimentally, isoprene was shown to increase the temperature at which thermal damage occurred by 10°C.<sup>44</sup> Computational studies for membranes containing isoprene identified a potential mechanism by which isoprene stabilized lipid tails, preventing the membrane from becoming too fluid at elevated temperature.<sup>45</sup> A later experimental study contested this hypothesis, pointing to no dependence on isoprene concentrations in liposome viscosity measurements at naturally occurring isoprene concentrations, but suggesting that isoprene may bind to thylakoid embedded proteins and modulate their dynamics.<sup>46</sup>

In this work, we investigated the dynamic properties and space requirement of lipids in a thylakoid membrane at different temperatures and different isoprene content using molecular dynamics simulations, and compare directly with prior simulation models.<sup>45</sup> The lipid-type decomposed temperature-dependent change in these properties provides insight into the required thylakoid compositional changes to try to keep the overall membrane properties constant. On the basis of the decomposed properties, we predict thylakoid properties for experimentally obtained lipid compositions at different temperatures to evaluate the changes in membrane properties after metabolic lipid composition adjustments.

## Methods

The broad simulation plan was to conduct classical molecular dynamics simulations for thylakoid membranes with and without isoprene at varying temperatures, and to compare these results with a fresh look at the model DMPC membrane used to measure the effect of isoprene in prior studies.<sup>45</sup> The details to implement this outline is presented below.

## Membrane Model

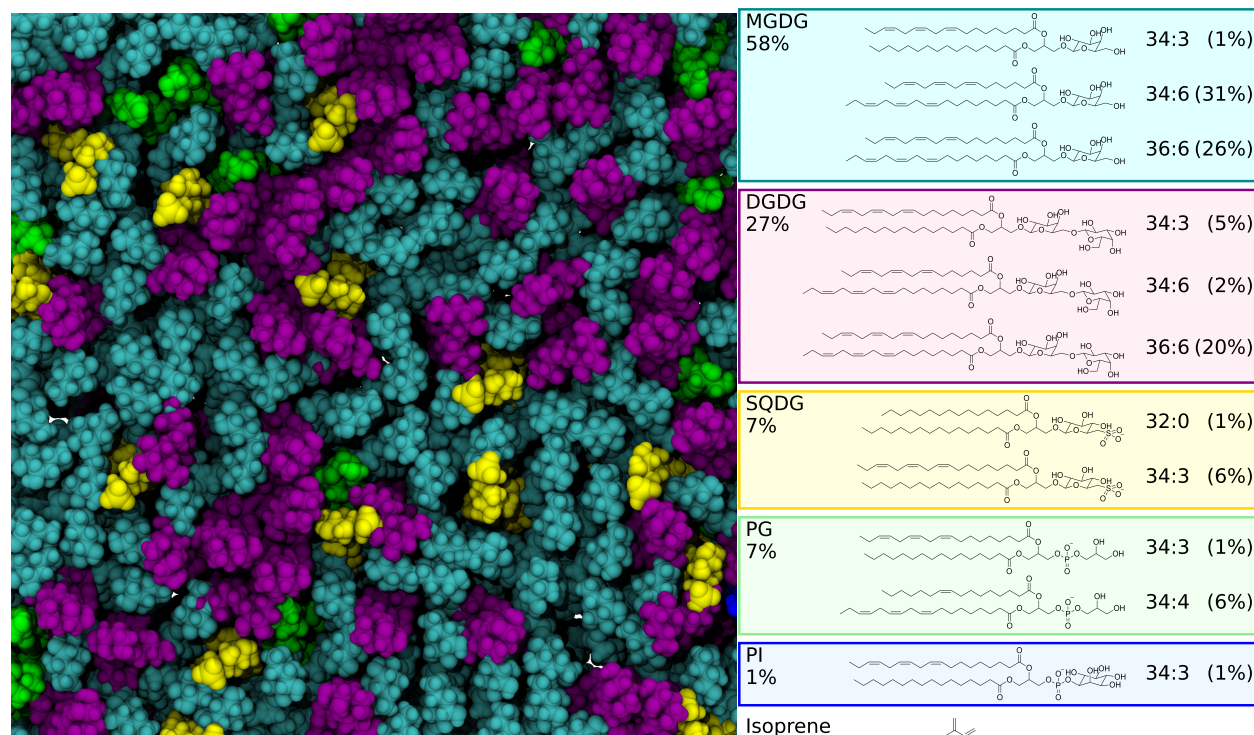


Figure 1: Initial thylakoid membrane structure at the beginning of the simulation. The membrane is comprised of *cyan* monogalactosyldiacylglycerol (MGDG), *purple* digalactosyldiacylglycerol (DGDG), *yellow* sulfoquinovosyl diacylglycerol (SQDG), *green* phosphatidylglycerol (PG), and *blue* phosphatidylinositol (PI). Either 0 or 20 mol-% isoprene were added to the composition.

All thylakoid membrane bilayers were built with the CHARMM-GUI membrane builder<sup>47,48</sup> using literature-derived lipid compositions for spinach thylakoids.<sup>4,5</sup> Both leaflets contained 198 lipids with 60 MGDG (18:3/16:3), 52 MGDG (18:3/18:3), 2 MGDG (16:0/18:3), 4 DGDG (18:3/16:3), 40 DGDG (18:3/18:3), 10 DGDG (16:0/18:3), 12 SQDG (16:0/18:3), 2 SQDG (16:0/16:0), 2 PG (16:0/18:3), 12 LYPG (18:3,16:1), 2 PI (16:3/18:3) lipids (Figure 1). The membrane surface was square with a size of  $10.9\text{ nm}^2 \times 10.9\text{ nm}^2$ . A pure DMPC bilayer with the same dimensions was also made in CHARMM-GUI, equivalent to the simulation design in prior research studying the effect of isoprene.<sup>45</sup> For each of the 9 temperatures from  $-3^\circ\text{C}$  to  $77^\circ\text{C}$  in  $10^\circ\text{C}$  steps, 5 membranes were generated with the same composition, but different starting positions of the lipids to reduce the bias introduced into the system by

our starting configuration. Each membrane was minimized and equilibrated in a NPT ensemble for 11.5 ns, before collecting the data for 400 ns in the same ensemble. Starting from the equilibrated membrane systems, 100 isoprene molecules (20 mol-% based on the number of lipid molecules) were introduced into the water phase of each system and the systems were equilibrated for another 10 ns, before 400 ns of data collection. During data collection, trajectory frames are written every nanosecond to enable detailed and statistically rigorous analysis.

## Molecular Dynamics Simulations

Molecular dynamics simulations were calculated with NAMD 3.0a9.<sup>49</sup> Lipids and ions force field parameters were defined by the CHARMM36m force field,<sup>50</sup> while water was described with the TIP3P model.<sup>51</sup> Isoprene was parameterized with CGenFF 2.4.0 using the CGenFF force field 4.4.<sup>52</sup> Periodic boundary conditions are applied to the system and intermolecular interactions are considered up to 12 Å with a switching function at 10 Å. Long-range electrostatic interactions are described by PME using a grid spacing of 1 Å.<sup>53</sup> The interaction pair list is generated every 100 steps within a cutoff of 14 Å. The temperature and pressure were maintained at 298 K and 1 bar, respectively, using a Langevin thermostat and barostat.<sup>54,55</sup> Langevin coupling coefficient was set to  $1.0 \text{ s}^{-1}$ , and the Langevin piston period and decay were set to 100, and 200, respectively. A semiisotropic barostat was applied to account for the different compressibility of the lipids and water molecules. All bonds to hydrogen are constraint with the SETTLE algorithm to the optimal length to enable 2 fs timesteps during simulation.<sup>56</sup>

## Analysis

VMD 1.9.4a55<sup>57</sup> and Python 3.8.5<sup>58</sup> are used to analyze the trajectories, leveraging in particular the numpy<sup>59</sup> and matplotlib<sup>60</sup> libraries. The time point in the trajectory at which the physical properties of the membrane no longer change with time is determined by the

area per lipid (Figure 4). After 200 ns, the area per lipid was constant for the remaining simulation time for all temperatures. The membrane properties were calculated between 200–400 ns and standard errors are estimated between the 5 membrane replicas.

## Area per Lipid

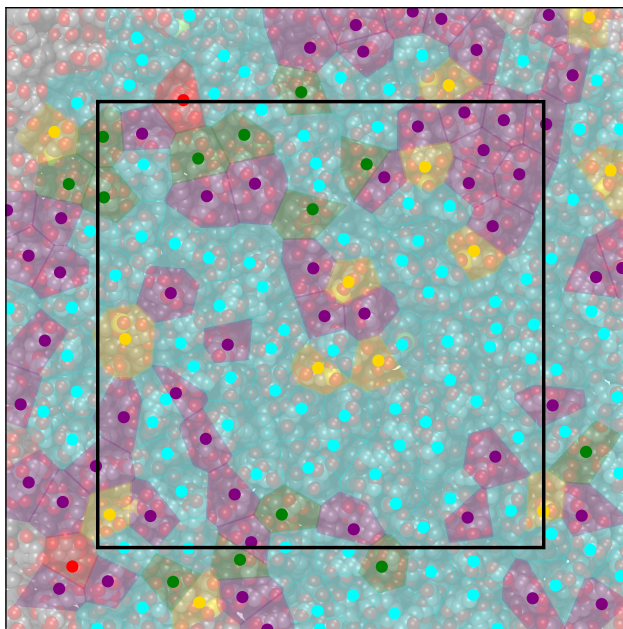


Figure 2: Top view upon the membrane surface with an overlaid voronoi diagram constructed from the  $C_1$ -glycerol atoms of each lipid. The different lipid types are colored with *cyan* MGDG, *purple* DGDG, *yellow* SQDG, *green* PG, and *red* PI. All voronoi cells with their points included in the black rectangular square are analyzed for the average area per lipid.

The average area per lipid ( $APL$ ) was calculated from the product of the  $xy$  membrane plane dimensions divided by the number of lipids  $N_L$  in one leaflet.

$$APL = \frac{x \times y}{N_L} \quad (1)$$

The surface area is decomposed into independent contributions of lipid types with the 2D voronoi algorithm utilizing the python implementation.<sup>61</sup> First, the membrane is centered to the system origin  $P(0,0)$ . In a second step, a 2D voronoi diagram is generated with the  $xy$  atom positions of the glycerol carbon that is connected to the phosphate or carbohydrate

head group as input. Subsequently, all voronoi cells with carbon atom positions that are not within a  $8 \text{ nm} \times 8 \text{ nm}$  square from the center point  $P(0,0)$  are omitted from further analysis (Figure 2). This avoids voronoi cells that have a common edge with the voronoi diagram border and thus an artificially high area. Third, the polygon areas of all voronoi cells that share a common lipid type are averaged. The surface area per lipid for an arbitrary composition is calculated by the weighted sum with respect to the lipid head type using the decomposed values for the respective temperature (Table S1).

### Order Parameter

Order parameters  $S_{\text{CH}}$  were calculated for all trajectories as the time-averaged angle  $\theta$  between the lipid tail C-H bonds and an assumed magnetic field parallel to the membrane plane normal in the z-direction.

$$S_{\text{CH}} = (3\cos^2\theta - 1) / 2 \tag{2}$$

The order parameter for the compositions from literature is calculated similarly to the area per lipid by the weighted sum of the decomposed values for lipid tail types (Table S1).

### Mass and Probability Density

Probability and mass densities of membrane components were determined along the membrane normal in z-direction with respect to the center of the membrane as the origin. The thickness of the membrane was calculated as the difference in z-position between the maximum glycerol mass density of the two membrane leaflets, equivalent to the hydrophobic thickness of the membrane, sometimes abbreviated  $D_c$ .<sup>62</sup> This metric was chosen since not all of our membrane components have phosphate groups. For decomposing the membrane thickness into specific lipids, the mass densities around the maxima were noisy and a Savitzky–Golay filter with a third order polynomial and a window size of 51 ( $10.2 \text{ \AA}$ ) was applied

to reduce the impact of limited statistics for single lipid types within the membrane.<sup>63</sup>

### Lateral Lipid Diffusion

Lateral diffusion coefficients for lipids within the membrane plane,  $D_{xy}$  were calculated from mean square displacements ( $MSD_{xy}$ ) over lag time  $t$  along the membrane surface plane of the glycerol carbons connected to the phosphate or carbohydrate oxygen atom.

$$D_{xy} = \frac{\Delta(MSD_{xy})}{4\Delta t} \quad (3)$$

This is the Einstein relation for two dimensional diffusion.<sup>64</sup> Following best practices,<sup>65</sup> linear regression was performed for data points between and including lag times 1 and 50 ns.

### Isoprene Permeability

Permeabilities were calculated by counting transition events  $E_t$  for the crossing of one isoprene molecule from the water phase through the membrane to the water phase on the other side:<sup>66</sup>

$$P = \frac{r}{2c_w} = \frac{E_t V_z}{2t_s N_w} \quad (4)$$

The transition rate  $r$  is calculated from the transition events  $E_t$  occurring over the simulation time  $t_s$  and the membrane surface area. The equilibrium isoprene concentration in the water phase  $c_w$  is the average number of isoprene molecules  $N_w$  divided by the water volume. Dividing the water volume by the membrane surface area gives the water height  $V_z$ . The description of a crossing is based on the definition of a membrane boundary that distinguishes between isoprene molecules that are inside or outside the membrane. In this study, we defined this boundary by the membrane thickness described above, padded by 5 Å and 1 Å for the thylakoid and DMPC membranes, respectively, to account for lipid head groups.

## Results

The thylakoid membrane and a reference DMPC membrane were simulated at nine different temperatures between  $-3^{\circ}\text{C}$  and  $77^{\circ}\text{C}$  in steps of  $10^{\circ}\text{C}$  (270-350 K). Although the membranes largely equilibrated within a few nanoseconds, lateral lipid diffusion was slow within the 400 ns sampling time, and thus the sampling is biased by the initial starting positions of the lipids. This bias was partially removed by simulating five replicas with different initial lipid positions for each membrane and temperature. The thickness, surface area, and measures of membrane structure and dynamics, were extracted from the molecular dynamics trajectories. The temperature dependence for these quantities is quantified in Figure 3. Qualitatively, the membrane surface area, volume per lipid, and lateral lipid diffusion increase with temperature, while the membrane thickness and order parameter decrease, irrespective of isoprene content.

In separate simulations, isoprene was added to the membrane systems and the changes in membrane properties were calculated (Figure 3). Isoprene quickly accumulates inside the membrane center and the glycerol layers, and diffuses only rarely into the aqueous phase (Figure S1,S2). The relatively high isoprene concentration consistently increases the membrane surface area. Since the trend between membrane thickness and isoprene was not consistent, the presence of isoprene effectively increased the total hydrophobic volume per lipid. Comparing the average dynamics, quantified by lateral diffusion coefficients or order parameters, even the high concentration of isoprene used within our simulation system did not elicit significant differences (Figure 3).

### Membrane Dimensions

As expected for complex and mixed membrane compositions, the lateral dimensions for the membrane are not fixed under changing temperatures, with lower temperatures leading to membrane compression while high temperatures led to membrane expansion for both

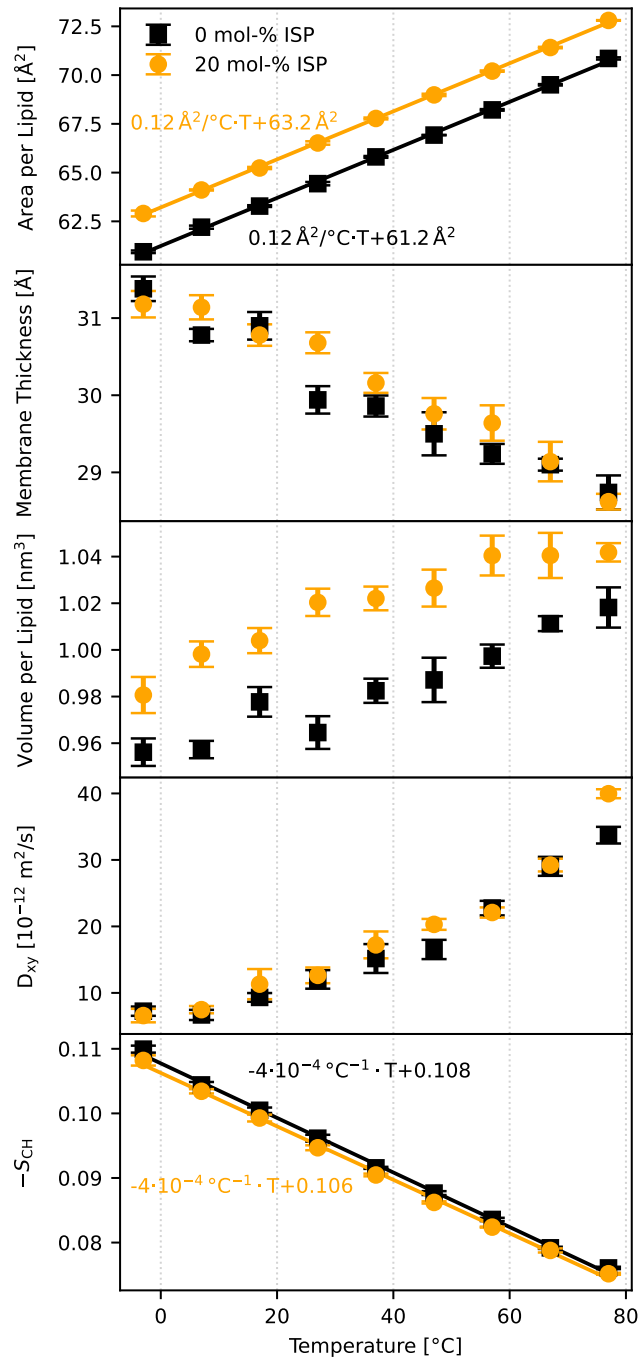


Figure 3: Temperature dependence of the thylakoid membrane dimensions, lateral lipid diffusion coefficient  $D_{xy}$ , and order parameter  $S_{CH}$  *black squares* without and *orange circles* with isoprene. Error bars indicate the standard errors.

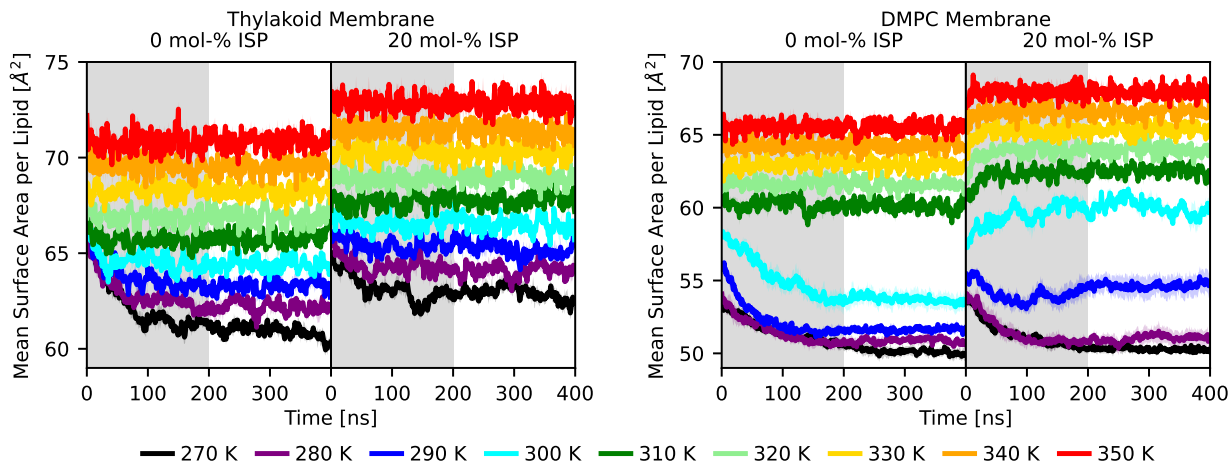


Figure 4: Area per lipid for the (left) thylakoid and (right) model membrane with 0 and 20 mol-% isoprene for different temperatures over the simulation time. The gray shaded areas indicate the first 200 ns equilibrating the membrane. Shaded colored regions around the line graphs indicate the standard error.

mixed thylakoid and single-component DMPC membrane compositions (Figure 4). For some membrane-temperature combinations, it could take up to 200 ns for the membrane dimensions to equilibrate around a mean value, and thus equilibrium properties reported in Figure 3 are only averaged over the last 200 ns of our simulation time. Even from the relatively crude quantification presented within Figure 4, we find that changing the temperature has a much stronger impact on membrane area than isoprene content, with the 12-15  $\text{\AA}^2$  per lipid range across temperatures far exceeding the 2-3  $\text{\AA}^2$  per lipid difference with and without isoprene. Where we do see a strong isoprene effect is the behavior for the 300 K trend in single component DMPC membranes, where the area per lipid shifts by over 5  $\text{\AA}^2$ . This reflects a change in the gel to liquid phase transition temperature for the DMPC bilayer, with isoprene fluidizing the membrane at temperature where it might otherwise form a gel phase.

For the thylakoid membrane, the membrane surface area rises linearly with temperature in the investigated temperature range by 1.2  $\text{\AA}^2$  every 10K (Figure 3). With 20 mol-% isoprene present in the system, the surface area increases independently of temperature by 2  $\text{\AA}^2$ . While these collective properties are reported in Figure 3, we find that not all lipids contribute equally to the temperature response. Instead, the area assigned to a specific lipid

as assigned by our Voronoi tessellation scheme varies based on the exact lipid type. We find that the type of lipid head group is the main influence on the amount of space that a lipid occupies inside the thylakoid membrane (Figure S3A). Phospholipid surface areas are in the same range as glycerolipid surface areas, as MGDG had the smallest area per lipid, whereas DGDG had the largest area per lipid. Within a class of lipid headgroups, the unsaturation and length of the tails had smaller impacts on membrane structure.

The thickness of the membrane, measured as the distance between glycerol moieties in the upper and lower leaflets, decreases with temperature (Figure 3). However, since the thickness decreases more slowly than the surface area increase, there is an overall increase in the hydrophobic volume for an individual lipid with increasing temperature (Figure 3). The thickness of the membrane depends on the head groups and tails of the lipids. The MGDG glycerol group is around 1 Å closer to the membrane center, compared to the other glycolipids DGDG and SQDG in a mixed system (Figure S3B). Lipids synthesized in the ER with tail combinations 16:0/18:3 or 16:0/16:0 result in thicker membranes than lipids synthesized in the chloroplast. In contrast, the highly unsaturated 18:3/18:3 lipids synthesized in the ER contributed to the membrane thickness similarly to lipids from the prokaryotic synthesis pathway. PI phospholipids commonly have signaling roles within cells. These lipids have the largest height from the membrane midplane (Figure S3B,C), sticking out and allowing interactions with peripheral proteins.

## Membrane Structure and Dynamics

The fluidity or order within the membrane structure can be determined from our simulations by measuring the membrane order parameter. The individual acyl tails within a thylakoid membrane demonstrate lower order with increasing temperature (Figure 3), with acyl tail saturation strongly influencing the order. Increasing the number of unsaturations decreases the order of the lipid tails (Figure S4). The length of the lipid tail, and particularly the position for lipid unsaturations dictate where the membrane is the most disordered. As has

been shown in other systems,<sup>67,68</sup> increasing acyl tail length and double bonds both reduce membrane ordering, increasing membrane fluidity. The ER-derived lipids with 16:0/18:3 and 16:0/16:0 acyl tails generally had a higher order at the end of their tails than the lipids synthesized in the chloroplast, which featured more unsaturation sites and thus disorder the membrane. Isoprene was not observed to influence the flexibility of the lipid tail, but it shifted the phase transition point of the DMPC membrane to lower temperatures (Figure S5), similar to what was observed based on area per lipid measurements. No phase transition to the gel phase was observed for the thylakoid membrane.

Lateral lipid diffusion within the membrane is 100 times slower than water self-diffusion, and increases with temperature (Figure 3). Measured diffusion coefficients for individual lipid types are all similar (Figure S6), indicating that diffusion is effectively homogeneous over these short simulation timescales where large-scale clustering cannot take place. Adding isoprene to the membrane did not noticeably increase or decrease lipid diffusion.

## Discussion

From the totality of the results, we find that isoprene, even at very high concentration, is alone not sufficient to counteract the impact of elevated temperature on thylakoid membranes. Our simulation results demonstrate that high isoprene concentrations only minimally influences membrane structure, increasing the area per lipid in a thylakoid membrane by the equivalent of a 15-20°C temperature increase. However, dynamical properties such as lateral lipid diffusion and membrane ordering are unchanged when isoprene is added (Figure 3). Similarly, the overall membrane thickness with and without isoprene remains relatively similar, suggesting that solving mismatched hydrophobic thicknesses for membrane proteins or altering membrane structure or dynamics directly is not the primary reason some plants emit isoprene.

Instead, perhaps isoprene is a signaling molecule that activates metabolic pathways<sup>69,70</sup>

that alter the membrane composition, thereby maintaining membrane homeostasis.<sup>71,72</sup> An important consideration is whether or not isoprene requires an active transport mechanism, as has been discussed for other volatile organic compounds.<sup>73,74</sup> Active transport is only effective when the inherent membrane permeability is low enough so that active transport is faster than passive diffusion, typically when the permeability coefficient is below  $10^{-6} \text{ cm s}^{-1}$ .<sup>75</sup> By measuring permeation events where isoprene transits the bilayer from within our simulations, we can estimate the isoprene permeability coefficient via Eq. 4. We find that the isoprene permeability for the thylakoid and DMPC membrane is  $1 - 10 \text{ cm s}^{-1}$  over the temperature range in the simulations suggesting passive transport as the favored transport mechanism (Figure S7). From prior simulations of lignin permeability under different membrane compositions,<sup>75,76</sup> as well as our comparison between thylakoid and DMPC membranes, we do not anticipate that isoprene transport would be dependent on active transport processes under any physiological conditions.

## Quantifying Temperature-Dependent Lipid Composition Changes *in vivo*

If the ratio between lipids were to change, that could conceivably alter membrane physical properties to counteract temperature-dependent changes within the membrane. For instance, replacing DGDG with MGDG at elevated temperature would reduce the overall increase in membrane surface area, but also make the hydrophobic region thinner (Figure S3). Within our simulations, we only consider a fixed membrane composition. However, by using the property decomposition alongside experimentally determined membrane compositions for *Arabidopsis* at different temperatures,<sup>77-82</sup> we can estimate what the overall membrane properties would be at these new compositions (Figure 5).

Figure 5 highlights the predicted response to changing temperature for two membrane structural properties, the area per lipid and the average order parameter. As shown in Figure 5, we find that the surface area per lipid for the lipid compositions within one study

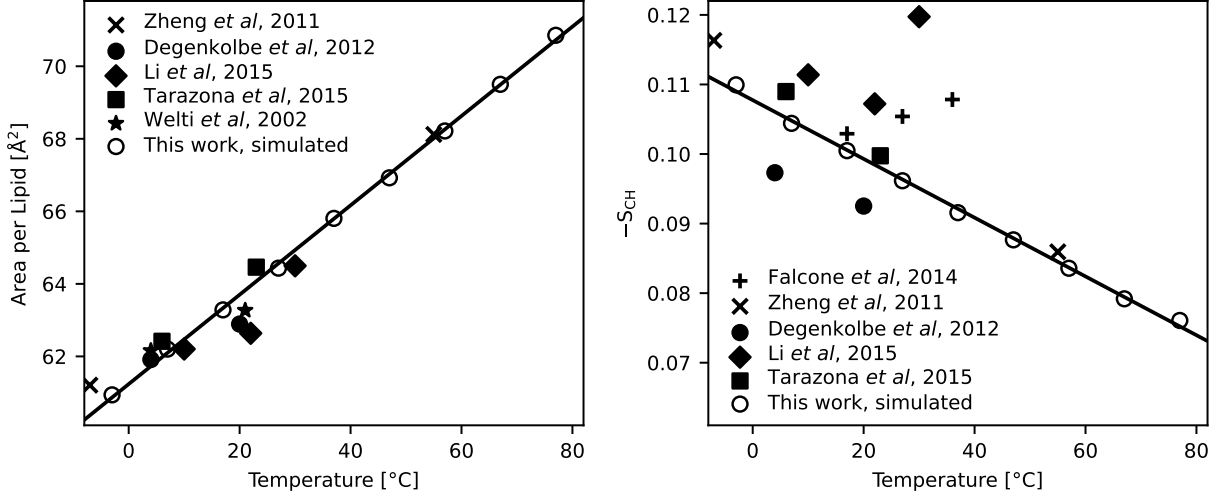


Figure 5: Area per lipid and order parameter for the lipid composition in this study (white circles) and other experimentally obtained lipid compositions at different temperatures. The two membrane properties for the lipid compositions not from this study were estimated with the weighted sum of the decomposed values for the lipid head group and tail types for area per lipid and order parameter, respectively (Table S1). Falcone et al.<sup>77</sup> only reported the lipid tail composition, while Welti et al.<sup>78</sup> only reported the lipid head composition. Consequently, their data is only present in one of the respective plots.

broadly follows the trend line for the simulated lipid composition used in this study, suggesting that the temperature induced compositional changes cannot arrest membrane expansion at elevated temperature. However, in the lipid compositions from Degenkolbe et al.,<sup>80</sup> Welti et al.,<sup>78</sup> and Li et al.,<sup>81</sup> the slope is clearly below the trend from the simulated membrane, and may indicate that the membrane changes are compensatory for increasing temperature. Observing the compensation effect in only three of five experimentally determined membrane compositions on its own is not statistically significant, and highlights the changes in membrane structure that would be expected over a day/night cycle where the temperatures can swing significantly.

Modulating the order parameter in response to temperature similarly shows a mixed trend. The compositions determined by Zheng et al.,<sup>79</sup> Tarazona et al.,<sup>82</sup> and Degenkolbe et al.<sup>80</sup> have slopes similar to the simulated static composition, suggesting that membrane composition changes do not influence lipid ordering. By contrast, Li et al.<sup>81</sup> and Falcone et al.<sup>77</sup> demonstrate clear deviations from the overall trend, with near-zero or even positive

slopes. Near-zero slopes for the tail order trend over a significant temperature range would clearly show membrane adaptation to a changing environment. Taken together, the evidence that isoprene directly mediates a response to elevated temperature by changing membrane properties is much weaker than that membrane composition is enzymatically modified, possibly triggered by isoprene binding or interaction with these enzymes.

## Chloroplast Membrane Responses to Temperature Changes

At high temperatures, the total volume of thylakoid membranes increases, with the membrane surface area strongly increasing, while the thylakoid membranes become only modestly thinner (Figure 3). This means that, in general, the volume of chloroplast membranes would increase at high temperature, consistent with experimentally observed swelling of mesophyll chloroplasts.<sup>83,84</sup> Further, in experiments it was found that the thylakoid grana destack at high temperatures.<sup>16,18</sup> It is possible that thinner but bulkier membranes are not able to maintain the same stacking arrangement, leading to a breakdown of the grana.

There are metabolic and organizational changes that help the plant deal with the extra thylakoid volume and thinner membranes. One is to transfer lipids from thylakoids to plastoglobuli, and experimentally the number of plastoglobuli increases significantly at high temperatures.<sup>83,85</sup> Furthermore, at high temperatures, plants increase the total contribution of lipids from the eukaryotic pathway.<sup>81,86</sup> Based on our data on the contribution of individual lipids to membrane thickness (Figure S3B), the transport of saturated 16:0/18:X ER lipids to the chloroplast can counteract decreasing membrane thickness at elevated temperatures, which decreases permeability and reduces the likelihood that protons leak through the membrane and waste the PMF generated by photosynthetic activity.

The volume of the membrane can be further reduced by converting DGDG to MGDG, which has a smaller surface area for interaction with its environment (Figure S3A). As a consequence for the smaller size of MGDG versus DGDG, a membrane enriched in MGDG would be thinner (Figure S3B). Experimentally, DGDG content is found to increase with

temperature.<sup>81,87–89</sup> As noted previously (Figure 5), estimating area per lipid values in a changing temperature environment based on reported lipid compositions<sup>78–82</sup> roughly follow the trend expected for a fixed membrane composition. At physiological temperatures, altering other membrane properties such as membrane thickness to reducing ion leakage may be better for the plant overall, thereby driving the exchange towards DGDG at elevated temperature.

At low temperatures, plants generally convert MGDG to DGDG depending on the plant species.<sup>37,81,90</sup> The higher surface area of DGDG (Figure S3B) mitigates the shrinking thylakoid volume at these temperatures. Although TGDG and TeDG were not measured in this study, we expect the surface area of TGDG to be higher than DGDG, allowing the plant to increase the surface area even further as needed to accommodate freezing temperatures.

Our simulated membranes follow the trends observed within the literature for decreasing thylakoid volume at low temperatures.<sup>24,25</sup> It is possible that the stroma thylakoids reduce in volume and cannot support the grana structure anymore, leading to dissociation of the grana thylakoid stacks from each other as previously reported.<sup>24,25</sup>

Beyond headgroups, desaturating lipid acyl tails is known to induce better thermotolerance,<sup>91</sup> and there is some evidence from our study that this may be a more active modification mechanism. Measures of the lipid order parameter, which quantifies in part the rigidity of the lipid tail, decreases with temperature and is much higher for unsaturated tails (Figure S5). Interestingly, our data suggest that saturated 16:0/18:X lipids from the eukaryotic synthesis pathway have lower flexibility than lipids produced in the chloroplast (Figure S4), supporting the argument that lipids are transferred from the ER to the chloroplast at high temperatures. The flexibility of the membrane gradually decreases with temperature, requiring increased lipid tail unsaturation at cold temperatures.<sup>17,92,93</sup> In the reverse of the response to elevated temperatures, it is beneficial at low temperatures to transport 16:0/18:X lipids synthesized by the eukaryotic pathway away from the thylakoid membrane, as they are more rigid than their prokaryotic counterpart (Figure S4). In wheat at low temperatures, the

total contribution of ER lipids compared to chloroplast lipids is reduced, supporting this argument.<sup>81</sup>

After adding isoprene to our model membranes, we find that isoprene localizes inside the thylakoid membrane, increasing surface area and lipid mobility, but not membrane thickness and rigidity, in contrast to previous simulation studies.<sup>45</sup> It should be noted that the simulation field has advanced tremendously since isoprene impacts on membranes were last investigated computationally, with substantially longer simulation times and better representations for the intermolecular interactions in membranes.<sup>94</sup> Indeed, given how much equilibration time was needed for our low temperature DMPC bilayers to settle into a consistent surface area per lipid (Figure 4), it is entirely possible that the 40 ns simulations previously conducted were never fully equilibrated. Using more modern force fields and the longer simulation times performed here yields results consistent with more recent experiments, which did not find a change in membrane viscosity after adding isoprene.<sup>46</sup>

## Conclusion

In summary, the spatial and dynamical properties of thylakoid membranes respond to changes in temperature. Thus, in order to maintain membrane homeostasis, plants must adapt their membranes to this changing environment. Based on our findings, plants likely do not make isoprene in response to elevated temperature as a membrane intercalating agent that would alter membrane properties. Instead, membrane modifications through enzymatic activity likely play a larger role in maintaining membrane homeostasis, balancing structural changes brought about via accelerated dynamics at high temperature. Through the computational microscope, we find that increased thylakoid membrane volume at elevated temperature may have its origins at the molecular scale, with implications for lipid trafficking within plant cells, as well as the spatial organization of lipids within chloroplasts by exchanging grana stacks for plastoglobuli.

## Supporting Information

Figures S1-S7 showing membrane cross-section mass and probability densities, permeabilities and decomposed membrane physical properties. Table S1. with decomposed values for the calculation of the order parameter and area per lipid in Figure 5.

## Acknowledgments

T.D.S, and J.V.V. are supported in part by the U.S. Department of Energy, Office of Basic Energy Sciences under grant number DE-FG02-91ER20021. This work used computational resources and services provided by the Institute for Cyber-Enabled Research at Michigan State University, and the Extreme Science and Engineering Discovery Environment project under project number TG-BIO210040, which is supported by National Science Foundation grant number ACI-1548562.<sup>95</sup>

## Notes

The authors declare no competing financial interest.

Data and Software Availability. Input files for the simulation systems, coordinate files during the simulation, and analysis scripts are available on Zenodo (<http://dx.doi.org/10.5281/zenodo.7565789>).

## References

- (1) Simkin, A. J.; López-Calcagno, P. E.; Raines, C. A. Feeding the World: Improving Photosynthetic Efficiency for Sustainable Crop Production. *Journal of Experimental Botany* **2019**, *70*, 1119–1140, DOI: 10.1093/jxb/ery445.
- (2) Koochak, H.; Puthiyaveetil, S.; Mullendore, D. L.; Li, M.; Kirchhoff, H. The Structural

- and Functional Domains of Plant Thylakoid Membranes. *Plant J* **2019**, *97*, 412–429, DOI: 10.1111/tpj.14127.
- (3) Ruban, A. V.; Johnson, M. P. Visualizing the Dynamic Structure of the Plant Photosynthetic Membrane. *Nature Plants* **2015**, *1*, 15161, DOI: 10.1038/nplants.2015.161.
- (4) Block, M. A.; Douce, R.; Joyard, J.; Rolland, N. Chloroplast Envelope Membranes: A Dynamic Interface between Plastids and the Cytosol. *Photosynth Res* **2007**, *92*, 225–244, DOI: 10.1007/s11120-007-9195-8.
- (5) Block, M. A.; Dorne, A. J.; Joyard, J.; Douce, R. Preparation and Characterization of Membrane Fractions Enriched in Outer and Inner Envelope Membranes from Spinach Chloroplasts. II. Biochemical Characterization. *Journal of Biological Chemistry* **1983**, *258*, 13281–13286, DOI: 10.1016/S0021-9258(17)44113-5.
- (6) Moellering, E. R.; Muthan, B.; Benning, C. Freezing Tolerance in Plants Requires Lipid Remodeling at the Outer Chloroplast Membrane. *Science* **2010**, *330*, 226–228, DOI: 10.1126/science.1191803.
- (7) Kobayashi, K. Role of Membrane Glycerolipids in Photosynthesis, Thylakoid Biogenesis and Chloroplast Development. *J Plant Res* **2016**, *129*, 565–580, DOI: 10.1007/s10265-016-0827-y.
- (8) Garab, G.; Ughy, B.; de Waard, P.; Akhtar, P.; Javornik, U.; Kotakis, C.; Šket, P.; Karlický, V.; Materová, Z.; Špunda, V.; Plavec, J.; van Amerongen, H.; Vígh, L.; As, H. V.; Lambrev, P. H. Lipid Polymorphism in Chloroplast Thylakoid Membranes – as Revealed by <sup>31</sup>P-NMR and Time-Resolved Merocyanine Fluorescence Spectroscopy. *Sci Rep* **2017**, *7*, 13343, DOI: 10.1038/s41598-017-13574-y.
- (9) Jouhet, J. Importance of the Hexagonal Lipid Phase in Biological Membrane Organization. *Front. Plant Sci.* **2013**, *4*, DOI: 10.3389/fpls.2013.00494.

- (10) Hagio, M.; Gombos, Z.; Várkonyi, Z.; Masamoto, K.; Sato, N.; Tsuzuki, M.; Wada, H. Direct Evidence for Requirement of Phosphatidylglycerol in Photosystem II of Photosynthesis. *Plant Physiology* **2000**, *124*, 795–804, DOI: 10.1104/pp.124.2.795.
- (11) Yu, B.; Benning, C. Anionic Lipids Are Required for Chloroplast Structure and Function in *Arabidopsis*. *The Plant Journal* **2003**, *36*, 762–770, DOI: 10.1046/j.1365-313X.2003.01918.x.
- (12) Bolik, S.; Albrieux, C.; Schneck, E.; Demé, B.; Jouhet, J. Sulfoquinovosyldiacylglycerol and Phosphatidylglycerol Bilayers Share Biophysical Properties and Are Good Mutual Substitutes in Photosynthetic Membranes. *Biochimica et Biophysica Acta (BBA) - Biomembranes* **2022**, *1864*, 184037, DOI: 10.1016/j.bbamem.2022.184037.
- (13) Hou, Q.; Ufer, G.; Bartels, D. Lipid Signalling in Plant Responses to Abiotic Stress: Lipid Signalling in Plant Responses to Abiotic Stress. *Plant, Cell & Environment* **2016**, *39*, 1029–1048, DOI: 10.1111/pce.12666.
- (14) Allen, D. K.; Bates, P. D.; Tjellström, H. Tracking the Metabolic Pulse of Plant Lipid Production with Isotopic Labeling and Flux Analyses: Past, Present and Future. *Progress in Lipid Research* **2015**, *58*, 97–120, DOI: 10.1016/j.plipres.2015.02.002.
- (15) LaBrant, E.; Barnes, A. C.; Roston, R. L. Lipid Transport Required to Make Lipids of Photosynthetic Membranes. *Photosynth Res* **2018**, *138*, 345–360, DOI: 10.1007/s11120-018-0545-5.
- (16) Mathur, S.; Agrawal, D.; Jajoo, A. Photosynthesis: Response to High Temperature Stress. *Journal of Photochemistry and Photobiology B: Biology* **2014**, *137*, 116–126, DOI: 10.1016/j.jphotobiol.2014.01.010.
- (17) Liu, X.; Zhou, Y.; Xiao, J.; Bao, F. Effects of Chilling on the Structure, Function and Development of Chloroplasts. *Front. Plant Sci.* **2018**, *9*, 1715, DOI: 10.3389/fpls.2018.01715.

- (18) Gounaris, K.; Brain, A.; Quinn, P.; Williams, W. Structural Reorganisation of Chloroplast Thylakoid Membranes in Response to Heat-Stress. *Biochimica et Biophysica Acta (BBA) - Bioenergetics* **1984**, *766*, 198–208, DOI: 10.1016/0005-2728(84)90232-9.
- (19) Sundby, C.; Melis, A.; Mäenpää, P.; Andersson, B. Temperature-Dependent Changes in the Antenna Size of Photosystem II. Reversible Conversion of Photosystem II $\alpha$  to Photosystem II $\beta$ . *Biochimica et Biophysica Acta (BBA) - Bioenergetics* **1986**, *851*, 475–483, DOI: 10.1016/0005-2728(86)90084-8.
- (20) Cao, J.; Govindjee, Chlorophyll a Fluorescence Transient as an Indicator of Active and Inactive Photosystem II in Thylakoid Membranes. *Biochimica et Biophysica Acta (BBA) - Bioenergetics* **1990**, *1015*, 180–188, DOI: 10.1016/0005-2728(90)90018-Y.
- (21) Ducruet, J.-M.; Lemoine, Y. Increased Heat Sensitivity of the Photosynthetic Apparatus in Triazine-Resistant Biotypes from Different Plant Species. *Plant and Cell Physiology* **1985**, *26*, 419–429, DOI: 10.1093/oxfordjournals.pcp.a076925.
- (22) Hu, S.; Ding, Y.; Zhu, C. Sensitivity and Responses of Chloroplasts to Heat Stress in Plants. *Front. Plant Sci.* **2020**, *11*, 375, DOI: 10.3389/fpls.2020.00375.
- (23) Schrader, S. M.; Wise, R. R.; Wacholtz, W. F.; Ort, D. R.; Sharkey, T. D. Thylakoid Membrane Responses to Moderately High Leaf Temperature in Pima Cotton. *Plant Cell Environ* **2004**, *27*, 725–735, DOI: 10.1111/j.1365-3040.2004.01172.x.
- (24) Kutík, J.; Holá, D.; Kočová, M.; Rothová, O.; Haisel, D.; Wilhelmová, N.; Tichá, I. Ultrastructure and Dimensions of Chloroplasts in Leaves of Three Maize (*Zea Mays* L.) Inbred Lines and Their F<sub>1</sub> Hybrids Grown Under Moderate Chilling Stress. *Photosynth.* **2004**, *42*, 447–455, DOI: 10.1023/B:PHOT.0000046165.15048.a4.
- (25) Holá, D.; Kutík, J.; Kočová, M.; Rothová, O. Low-Temperature Induced Changes in the Ultrastructure of Maize Mesophyll Chloroplasts Strongly Depend on the Chilling

- Pattern/Intensity and Considerably Differ among Inbred and Hybrid Genotypes. *Photosynth.* **2008**, *46*, DOI: 10.1007/s11099-008-0061-5.
- (26) Venzhik, Y. V.; Titov, A. F.; Talanova, V. V.; Miroslavov, E. A. Ultrastructure and Functional Activity of Chloroplasts in Wheat Leaves under Root Chilling. *Acta Physiol Plant* **2014**, *36*, 323–330, DOI: 10.1007/s11738-013-1413-8.
- (27) Saropulos, A. S.; Drennan, D. S. H. Ultrastructural Alterations in Mesophyll and Bundle Sheath Chloroplasts of Two Maize Cultivars in Response to Chilling at High Irradiance. *Biologia plant.* **2007**, *51*, 690–698, DOI: 10.1007/s10535-007-0144-3.
- (28) Karim, S.; Alezzawi, M.; Garcia-Petit, C.; Solymosi, K.; Khan, N. Z.; Lindquist, E.; Dahl, P.; Hohmann, S.; Aronsson, H. A Novel Chloroplast Localized Rab GT-Pase Protein CPRabA5e Is Involved in Stress, Development, Thylakoid Biogenesis and Vesicle Transport in Arabidopsis. *Plant Mol Biol* **2014**, *84*, 675–692, DOI: 10.1007/s11103-013-0161-x.
- (29) Musser, R. L.; Thomas, S. A.; Wise, R. R.; Peeler, T. C.; Naylor, A. W. Chloroplast Ultrastructure, Chlorophyll Fluorescence, and Pigment Composition in Chilling-Stressed Soybeans. *Plant Physiol.* **1984**, *74*, 749–754, DOI: 10.1104/pp.74.4.749.
- (30) Zbierzak, A. M.; Porfirova, S.; Griebel, T.; Melzer, M.; Parker, J. E.; Dörmann, P. A TIR-NBS Protein Encoded by Arabidopsis *Chilling Sensitive 1* ( *CHS1* ) Limits Chloroplast Damage and Cell Death at Low Temperature. *Plant J* **2013**, *75*, 539–552, DOI: 10.1111/tpj.12219.
- (31) Koynova, R.; Tenchov, B. In *Encyclopedia of Biophysics*; Roberts, G. C. K., Ed.; Springer Berlin Heidelberg: Berlin, Heidelberg, 2013; pp 1841–1854, DOI: 10.1007/978-3-642-16712-6\_542.
- (32) Fujikawa, S. Artificial Biological Membrane Ultrastructural Changes

- Caused by Freezing. *Electron Microscopy Reviews* **1988**, *1*, 113–140, DOI: 10.1016/S0892-0354(98)90008-9.
- (33) Li, R.; Mitra, N.; Gratkowski, H.; Vilaire, G.; Litvinov, R.; Nagasami, C.; Weisel, J. W.; Lear, J. D.; Degrado, W. F.; Bennett, J. S. Activation of Integrin  $\alpha$ IIb $\beta$ 3 by Modulation of Transmembrane Helix Associations. *Science (80-. )*. **2003**, *300*, 795–798, DOI: 10.1126/science.1079441.
- (34) Gruszecki, W. I.; Strzałka, K. Carotenoids as Modulators of Lipid Membrane Physical Properties. *Biochimica et Biophysica Acta (BBA) - Molecular Basis of Disease* **2005**, *1740*, 108–115, DOI: 10.1016/j.bbadis.2004.11.015.
- (35) Szilágyi, A.; Selstam, E.; Åkerlund, H.-E. Laurdan Fluorescence Spectroscopy in the Thylakoid Bilayer: The Effect of Violaxanthin to Zeaxanthin Conversion on the Galactolipid Dominated Lipid Environment. *Biochimica et Biophysica Acta (BBA) - Biomembranes* **2008**, *1778*, 348–355, DOI: 10.1016/j.bbamem.2007.10.006.
- (36) Zheng, G.; Li, L.; Li, W. Glycerolipidome Responses to Freezing- and Chilling-Induced Injuries: Examples in Arabidopsis and Rice. *BMC Plant Biol* **2016**, *16*, 70, DOI: 10.1186/s12870-016-0758-8.
- (37) Kenchanmane Raju, S. K.; Barnes, A. C.; Schnable, J. C.; Roston, R. L. Low-Temperature Tolerance in Land Plants: Are Transcript and Membrane Responses Conserved? *Plant Science* **2018**, *276*, 73–86, DOI: 10.1016/j.plantsci.2018.08.002.
- (38) Skupień, J.; Wójtowicz, J.; Kowalewska, Ł.; Mazur, R.; Garstka, M.; Gieczewska, K.; Mostowska, A. Dark-Chilling Induces Substantial Structural Changes and Modifies Galactolipid and Carotenoid Composition during Chloroplast Biogenesis in Cucumber ( *Cucumis Sativus* L.) Cotyledons. *Plant Physiology and Biochemistry* **2017**, *111*, 107–118, DOI: 10.1016/j.plaphy.2016.11.022.

- (39) Sharkey, T. D.; Yeh, S. I. ISOPRENE EMISSION FROM PLANTS. *Annu. Rev. Plant. Physiol. Plant. Mol. Biol.* **2001**, *52*, 407–436, DOI: 10.1146/annurev.arplant.52.1.407.
- (40) Mayrhofer, S.; Teuber, M.; Zimmer, I.; Louis, S.; Fischbach, R. J.; Schnitzler, J.-P. Diurnal and Seasonal Variation of Isoprene Biosynthesis-Related Genes in Grey Poplar Leaves. *Plant Physiology* **2005**, *139*, 474–484, DOI: 10.1104/pp.105.066373.
- (41) Sharkey, T. D.; Singaas, E. L. Why Plants Emit Isoprene. *Nature* **1995**, *374*, 769–769, DOI: 10.1038/374769a0.
- (42) Sharkey, T. D.; Wiberley, A. E.; Donohue, A. R. Isoprene Emission from Plants: Why and How. *Annals of Botany* **2007**, *101*, 5–18, DOI: 10.1093/aob/mcm240.
- (43) Tattini, M.; Velikova, V.; Vickers, C.; Brunetti, C.; Di Ferdinando, M.; Trivellini, A.; Fineschi, S.; Agati, G.; Ferrini, F.; Loreto, F. Isoprene Production in Transgenic Tobacco Alters Isoprenoid, Non-Structural Carbohydrate and Phenylpropanoid Metabolism, and Protects Photosynthesis from Drought Stress: Isoprene Emission and Plant Metabolism under Drought Stress. *Plant Cell Environ* **2014**, *37*, 1950–1964, DOI: 10.1111/pce.12350.
- (44) Singaas, E. L.; Lerdau, M.; Winter, K.; Sharkey, T. D. Isoprene Increases Thermotolerance of Isoprene-Emitting Species. *Plant Physiol.* **1997**, *115*, 1413–1420, DOI: 10.1104/pp.115.4.1413.
- (45) Siwko, M. E.; Marrink, S. J.; de Vries, A. H.; Kozubek, A.; Schoot Uiterkamp, A. J.; Mark, A. E. Does Isoprene Protect Plant Membranes from Thermal Shock? A Molecular Dynamics Study. *Biochim. Biophys. Acta - Biomembr.* **2007**, *1768*, 198–206, DOI: 10.1016/j.bbamem.2006.09.023.
- (46) Harvey, C. M.; Li, Z.; Tjellström, H.; Blanchard, G. J.; Sharkey, T. D. Concentration

- of Isoprene in Artificial and Thylakoid Membranes. *J. Bioenerg. Biomembr.* **2015**, *47*, 419–429, DOI: 10.1007/s10863-015-9625-9.
- (47) Wu, E. L.; Cheng, X.; Jo, S.; Rui, H.; Song, K. C.; Dávila-Contreras, E. M.; Qi, Y.; Lee, J.; Monje-Galvan, V.; Venable, R. M.; Klauda, J. B.; Im, W. CHARMM-GUI Membrane Builder toward Realistic Biological Membrane Simulations. *J. Comput. Chem.* **2014**, *35*, 1997–2004, DOI: 10.1002/jcc.23702.
- (48) Jo, S.; Kim, T.; Iyer, V. G.; Im, W. CHARMM-GUI: A Web-Based Graphical User Interface for CHARMM. *J. Comput. Chem.* **2008**, *29*, 1859–1865, DOI: 10.1002/jcc.20945.
- (49) Phillips, J. C. et al. Scalable Molecular Dynamics on CPU and GPU Architectures with NAMD. *J. Chem. Phys.* **2020**, *153*, 44130, DOI: 10.1063/5.0014475.
- (50) Huang, J.; Rauscher, S.; Nawrocki, G.; Ran, T.; Feig, M.; De Groot, B. L.; Grubmüller, H.; MacKerell, A. D. CHARMM36m: An Improved Force Field for Folded and Intrinsically Disordered Proteins. *Nat. Methods* **2016**, *14*, 71–73, DOI: 10.1038/nmeth.4067.
- (51) Jorgensen, W. L.; Chandrasekhar, J.; Madura, J. D.; Impey, R. W.; Klein, M. L. Comparison of Simple Potential Functions for Simulating Liquid Water. *J. Chem. Phys.* **1983**, *79*, 926–935, DOI: 10.1063/1.445869.
- (52) Vanommeslaeghe, K.; Hatcher, E.; Acharya, C.; Kundu, S.; Zhong, S.; Shim, J.; Darian, E.; Guvench, O.; Lopes, P.; Vorobyov, I.; Mackerell, A. D. CHARMM General Force Field: A Force Field for Drug-like Molecules Compatible with the CHARMM All-Atom Additive Biological Force Fields. *J. Comput. Chem.* **2009**, NA–NA, DOI: 10.1002/jcc.21367.
- (53) Essmann, U.; Perera, L.; Berkowitz, M. L.; Darden, T.; Lee, H.; Pedersen, L. G. A

- Smooth Particle Mesh Ewald Method. *J. Chem. Phys.* **1995**, *103*, 8577–8593, DOI: 10.1063/1.470117.
- (54) Grest, G. S.; Kremer, K. Molecular Dynamics Simulation for Polymers in the Presence of a Heat Bath. *Phys. Rev. A* **1986**, *33*, 3628–3631, DOI: 10.1103/PhysRevA.33.3628.
- (55) Feller, S. E.; Zhang, Y.; Pastor, R. W.; Brooks, B. R. Constant Pressure Molecular Dynamics Simulation: The Langevin Piston Method. *J. Chem. Phys.* **1995**, *103*, 4613–4621, DOI: 10.1063/1.470648.
- (56) Miyamoto, S.; Kollman, P. A. Settle: An Analytical Version of the SHAKE and RATTLE Algorithm for Rigid Water Models. *J. Comput. Chem.* **1992**, *13*, 952–962, DOI: 10.1002/jcc.540130805.
- (57) Humphrey, W.; Dalke, A.; Schulten, K. VMD - Visual Molecular Dynamics. *J. Mol. Graph.* **1996**, *14*, 33–38, DOI: 10.1016/0263-7855(96)00018-5.
- (58) Van Rossum, G.; Drake, F. L. *Python 3 Reference Manual*; CreateSpace: Scotts Valley, CA, 2009.
- (59) Harris, C. R. et al. Array Programming with NumPy. *Nature* **2020**, *585*, 357–362, DOI: 10.1038/s41586-020-2649-2.
- (60) Hunter, J. D. Matplotlib: A 2D Graphics Environment. *Comput. Sci. Eng.* **2007**, *9*, 90–95, DOI: 10.1109/MCSE.2007.55.
- (61) Virtanen, P. et al. SciPy 1.0: Fundamental Algorithms for Scientific Computing in Python. *Nat. Methods* **2020**, *17*, 261–272, DOI: 10.1038/s41592-019-0686-2.
- (62) Nagle, J. F.; Tristram-Nagle, S. Structure of Lipid Bilayers. *Biochim. Biophys. Acta - Rev. Biomembr.* **2000**, *1469*, 159–195, DOI: [http://dx.doi.org/10.1016/S0304-4157\(00\)00016-2](http://dx.doi.org/10.1016/S0304-4157(00)00016-2).

- (63) Savitzky, A.; Golay, M. J. E. Smoothing and Differentiation of Data by Simplified Least Squares Procedures. *Anal. Chem.* **1964**, *36*, 1627–1639, DOI: 10.1021/ac60214a047.
- (64) Einstein, A. Über Die von Der Molekularkinetischen Theorie Der Wärme Geforderte Bewegung von in Ruhenden Flüssigkeiten Suspendierten Teilchen. *Ann. Phys.* **1905**, *322*, 549–560, DOI: 10.1002/andp.19053220806.
- (65) Maginn, E. J.; Messerly, R. A.; Carlson, D. J.; Roe, D. R.; Elliot, J. R. Best Practices for Computing Transport Properties 1. Self-Diffusivity and Viscosity from Equilibrium Molecular Dynamics [Article v1.0]. *LiveCoMS* **2020**, *2*, DOI: 10.33011/livecoms.1.1.6324.
- (66) Venable, R. M.; Krämer, A.; Pastor, R. W. Molecular Dynamics Simulations of Membrane Permeability. *Chem. Rev.* **2019**, *119*, 5954–5997, DOI: 10.1021/acs.chemrev.8b00486.
- (67) Niemelä, P. S.; Hyvönen, M. T.; Vattulainen, I. Influence of Chain Length and Unsaturation on Sphingomyelin Bilayers. *Biophysical Journal* **2006**, *90*, 851–863, DOI: 10.1529/biophysj.105.067371.
- (68) Zhuang, X.; Dávila-Contreras, E. M.; Beaven, A. H.; Im, W.; Klauda, J. B. An Extensive Simulation Study of Lipid Bilayer Properties with Different Head Groups, Acyl Chain Lengths, and Chain Saturations. *Biochimica et Biophysica Acta (BBA) - Biomembranes* **2016**, *1858*, 3093–3104, DOI: 10.1016/j.bbamem.2016.09.016.
- (69) Zuo, Z.; Weraduwege, S. M.; Lantz, A. T.; Sanchez, L. M.; Weise, S. E.; Wang, J.; Childs, K. L.; Sharkey, T. D. Isoprene Acts as a Signaling Molecule in Gene Networks Important for Stress Responses and Plant Growth. *Plant Physiol.* **2019**, *180*, 124–152, DOI: 10.1104/pp.18.01391.
- (70) Weraduwege, S. M.; Sahu, A.; Kulke, M.; Vermaas, J. V.; Sharkey, T. D. Characteriza-

tion of Promoter Elements of Isoprene-Responsive Genes, and the Ability of Isoprene to Bind START Domain Transcription Factors. *Plant Direct* **2023**, *forthcoming*.

- (71) Martinière, A.; Shvedunova, M.; Thomson, A. J.; Evans, N. H.; Penfield, S.; Runions, J.; McWatters, H. G. Homeostasis of Plasma Membrane Viscosity in Fluctuating Temperatures. *New Phytologist* **2011**, *192*, 328–337, DOI: 10.1111/j.1469-8137.2011.03821.x.
- (72) Zheng, Y.; Yang, Y.; Wang, M.; Hu, S.; Wu, J.; Yu, Z. Differences in Lipid Homeostasis and Membrane Lipid Unsaturation Confer Differential Tolerance to Low Temperatures in Two Cycas Species. *BMC Plant Biol* **2021**, *21*, 377, DOI: 10.1186/s12870-021-03158-4.
- (73) Widhalm, J. R.; Jaini, R.; Morgan, J. A.; Dudareva, N. Rethinking How Volatiles Are Released from Plant Cells. *Trends in Plant Science* **2015**, *20*, 545–550, DOI: 10.1016/j.tplants.2015.06.009.
- (74) Adebessin, F. et al. Emission of Volatile Organic Compounds from Petunia Flowers Is Facilitated by an ABC Transporter. *Science* **2017**, *356*, 1386–1388, DOI: 10.1126/science.aan0826.
- (75) Vermaas, J. V.; Dixon, R. A.; Chen, F.; Mansfield, S. D.; Boerjan, W.; Ralph, J.; Crowley, M. F.; Beckham, G. T. Passive Membrane Transport of Lignin-Related Compounds. *Proc. Natl. Acad. Sci. U.S.A.* **2019**, *116*, 23117–23123, DOI: 10.1073/pnas.1904643116.
- (76) Vermaas, J. V.; Crowley, M. F.; Beckham, G. T. Molecular Simulation of Lignin-Related Aromatic Compound Permeation through Gram-Negative Bacterial Outer Membranes. *Journal of Biological Chemistry* **2022**, *298*, 102627, DOI: 10.1016/j.jbc.2022.102627.

- (77) Falcone, D. L.; Ogas, J. P.; Somerville, C. R. Regulation of Membrane Fatty Acid Composition by Temperature in Mutants of Arabidopsis with Alterations in Membrane Lipid Composition. *BMC Plant Biol* **2004**, *4*, 17, DOI: 10.1186/1471-2229-4-17.
- (78) Welte, R.; Li, W.; Li, M.; Sang, Y.; Biesiada, H.; Zhou, H.-E.; Rajashekar, C.; Williams, T. D.; Wang, X. Profiling Membrane Lipids in Plant Stress Responses. *Journal of Biological Chemistry* **2002**, *277*, 31994–32002, DOI: 10.1074/jbc.M205375200.
- (79) Zheng, G.; Tian, B.; Zhang, F.; Tao, F.; Li, W. Plant Adaptation to Frequent Alterations between High and Low Temperatures: Remodelling of Membrane Lipids and Maintenance of Unsaturation Levels: Lipid Changes in High-Low Temperature Alteration. *Plant, Cell & Environment* **2011**, *34*, 1431–1442, DOI: 10.1111/j.1365-3040.2011.02341.x.
- (80) Degenkolbe, T.; Giavalisco, P.; Zuther, E.; Seiwert, B.; Hinch, D. K.; Willmitzer, L. Differential Remodeling of the Lipidome during Cold Acclimation in Natural Accessions of *Arabidopsis Thaliana*: Lipidomics of Arabidopsis Cold Acclimation. *The Plant Journal* **2012**, *72*, 972–982, DOI: 10.1111/tpj.12007.
- (81) Li, Q.; Zheng, Q.; Shen, W.; Cram, D.; Fowler, D. B.; Wei, Y.; Zou, J. Understanding the Biochemical Basis of Temperature-Induced Lipid Pathway Adjustments in Plants. *The Plant Cell* **2015**, *27*, 86–103, DOI: 10.1105/tpc.114.134338.
- (82) Tarazona, P.; Feussner, K.; Feussner, I. An Enhanced Plant Lipidomics Method Based on Multiplexed Liquid Chromatography-Mass Spectrometry Reveals Additional Insights into Cold- and Drought-Induced Membrane Remodeling. *Plant J* **2015**, *84*, 621–633, DOI: 10.1111/tpj.13013.
- (83) Zhang, R.; Wise, R. R.; Struck, K. R.; Sharkey, T. D. Moderate Heat Stress of Arabidopsis Thaliana Leaves Causes Chloroplast Swelling and Plastoglobule Formation. *Photosynth Res* **2010**, *105*, 123–134, DOI: 10.1007/s11120-010-9572-6.

- (84) Anderson, C. M. et al. High Light and Temperature Reduce Photosynthetic Efficiency through Different Mechanisms in the C4 Model *Setaria Viridis*. *Commun Biol* **2021**, *4*, 1092, DOI: 10.1038/s42003-021-02576-2.
- (85) Yuan, L.; Yuan, Y.; Liu, S.; Wang, J.; Zhu, S.; Chen, G.; Hou, J.; Wang, C. Influence of High Temperature on Photosynthesis, Antioxidative Capacity of Chloroplast, and Carbon Assimilation among Heat-tolerant and Heat-susceptible Genotypes of Nonheading Chinese Cabbage. *horts* **2017**, *52*, 1464–1470, DOI: 10.21273/HORTSCI12259-17.
- (86) Zoong Lwe, Z.; Sah, S.; Persaud, L.; Li, J.; Gao, W.; Raja Reddy, K.; Narayanan, S. Alterations in the Leaf Lipidome of *Brassica Carinata* under High-Temperature Stress. *BMC Plant Biol* **2021**, *21*, 404, DOI: 10.1186/s12870-021-03189-x.
- (87) Su, K.; Bremer, D. J.; Jeannotte, R.; Welti, R.; Yang, C. Membrane Lipid Composition and Heat Tolerance in Cool-season Turfgrasses, Including a Hybrid Bluegrass. *J. Amer. Soc. Hort. Sci.* **2009**, *134*, 511–520, DOI: 10.21273/JASHS.134.5.511.
- (88) Chen, J.; Burke, J. J.; Xin, Z.; Xu, C.; Velten, J. Characterization of the Arabidopsis Thermosensitive Mutant Atts02 Reveals an Important Role for Galactolipids in Thermotolerance. *Plant Cell Environ* **2006**, *29*, 1437–1448, DOI: 10.1111/j.1365-3040.2006.01527.x.
- (89) Süß, K.-H.; Yordanov, I. T. Biosynthetic Cause of *in Vivo* Acquired Thermotolerance of Photosynthetic Light Reactions and Metabolic Responses of Chloroplasts to Heat Stress. *Plant Physiol.* **1986**, *81*, 192–199, DOI: 10.1104/pp.81.1.192.
- (90) Gu, Y.; He, L.; Zhao, C.; Wang, F.; Yan, B.; Gao, Y.; Li, Z.; Yang, K.; Xu, J. Biochemical and Transcriptional Regulation of Membrane Lipid Metabolism in Maize Leaves under Low Temperature. *Front. Plant Sci.* **2017**, *8*, 2053, DOI: 10.3389/fpls.2017.02053.

- (91) Pranneshraj, V.; Sangha, M. K.; Djalovic, I.; Miladinovic, J.; Djanaguiraman, M. Lipidomics-Assisted GWAS (IGWAS) Approach for Improving High-Temperature Stress Tolerance of Crops. *IJMS* **2022**, *23*, 9389, DOI: 10.3390/ijms23169389.
- (92) Khodakovskaya, M.; McAvoy, R.; Peters, J.; Wu, H.; Li, Y. Enhanced Cold Tolerance in Transgenic Tobacco Expressing a Chloroplast  $\omega$ -3 Fatty Acid Desaturase Gene under the Control of a Cold-Inducible Promoter. *Planta* **2006**, *223*, 1090–1100, DOI: 10.1007/s00425-005-0161-4.
- (93) Popov, V. N.; Antipina, O. V.; Pchelkin, V. P.; Tsydendambaev, V. D. Changes in Fatty Acid Composition of Lipids in Chloroplast Membranes of Tobacco Plants during Cold Hardening. *Russ J Plant Physiol* **2017**, *64*, 156–161, DOI: 10.1134/S1021443717010137.
- (94) Klauda, J. B.; Venable, R. M.; Freites, J. A.; O'Connor, J. W.; Tobias, D. J.; Mondragon-Ramirez, C.; Vorobyov, I.; MacKerell, A. D.; Pastor, R. W. Update of the CHARMM All-Atom Additive Force Field for Lipids: Validation on Six Lipid Types. *J. Phys. Chem. B* **2010**, *114*, 7830–7843, DOI: 10.1021/jp101759q.
- (95) Towns, J.; Cockerill, T.; Dahan, M.; Foster, I.; Gaither, K.; Grimshaw, A.; Hazelwood, V.; Lathrop, S.; Lifka, D.; Peterson, G. D.; Roskies, R.; Scott, J. R.; Wilkins-Diehr, N. XSEDE: Accelerating Scientific Discovery. *Comput. Sci. Eng.* **2014**, *16*, 62–74, DOI: 10.1109/MCSE.2014.80.